Spark plasma reaction sintering of ZrO2-mullite composites from plasma spheroidized zircon/alumina powders

Yu, L. G.; Li, Y.; Munir, Z. A.; Khor, Khiam Aik; Dong, Zhili

2003

Khor, K. A., Yu, L. G., Li, Y., Dong, Z. L., & Munic, Z. A. (2003). Spark Plasma Reaction Sintering of ZrO2-mullite Composites from Plasma Spheroidized Zircon/alumina Powders. Materials Science and Engineering A, 339(1-2), 286-296.

https://hdl.handle.net/10356/97176

https://doi.org/10.1016/S0921-5093(02)00151-X

Spark plasma reaction sintering of ZrO_2 —mullite composites from plasma spheroidized zircon/alumina powders

K. A. Khor [a,], L. G. Yu[a], Y. Li[b], Z. L. Dong[b], Z. A. Munir[c]*

[a] *School of Mechanical and Production Engineering, Nanyang Technological University, 50 Nanyang Avenue, Singapore 639798, Singapore*
[b] *Environmental Technology Institute, Innovation Centre, Block 2 Unit 237, 18 Nanyang Drive, Singapore 637723, Singapore*
[c] *College of Engineering, University of California, Davis, One Shields Avenue, Davis, CA 95616, USA*
[*] *Corresponding author. E-mail address: mkakhor@ntu.edu.sg*

ABSTRACT

Mullite-zirconia ceramic composites are prepared by reaction sintering of plasma spheroidized (PS) zircon-alumina powders in a spark plasma sintering (SPS) system at 1000, 1100, 1200 and 1300 ℃ with duration of 10 and 30 min. At SPS temperature of 1000 ℃, evidence of zircon decomposition is detected, while at 1200 ℃, mullite formation dominates the process, resulting in significant increases in microhardness, Young's modulus and fracture toughness values. At SPS temperature of 1300 ℃, due to recrystallization, rapid grain growth, and intergranular micro cracking, there is a slight decrease of microhardness and Young's modulus values. Yet, fracture toughness as high as 11.2±1.1 MPa $m^{1/2}$ is obtained by the indentation technique. The results indicate that with optimized sintering parameters, a combination of PS and SPS is effective in preparing high performance mullite/ZrO_2 composites from zircon/alumina mixtures at a relatively low reaction sintering temperature.

Keywords: Spark plasma sintering; Zircon alumina mixtures; Mullite zirconia composites; Microstructure; Young's modulus; Fracture toughness; Reaction sintering

1. INTRODUCTION

Mullite has attracted considerable attention in the last decade due to its high melting point, chemical stability, low thermal expansion, high creep and thermal shock resistance, and attractive bending strength at high temperatures [1-3]. Moreover, with a dielectric constant of 6.7, mullite-based microelectronics substrate can result in about 17% lower signal transmission delay time than an alumina substrate (with a dielectric constant of 9.8). As a result, mullite and mullite-based glass-ceramics have been considered as one of the most important candidate for high performance packaging applications [4-6]. However, the low fracture toughness of mullite and, the difficulties in sintering to full

density are the main obstacles for mullite materials from more widespread engineering applications.

Introducing ZrO_2 as reinforcement in the mullite matrix [7] can however, enhance the toughness of mullite. Various processing routes [8-14] can prepare ZrO2-mullite composites. Reaction sintering of zircon and Al_2O_3 is a relatively simple and inexpensive route to obtain homogeneous mullite-zirconia ceramics with enhanced mechanical properties. Table 1 gives a comparison of the mechanical properties of mullite, zirconia and alumina. Claussen et al. [7] reported that the fracture toughness of mullite/ZrO2 prepared by reaction sintering of zircon/Al_2O_3 can attain 4.5 ± 0.3 MPa $m^{1/2}$. It is accomplished by the following reaction at a temperature around 1500 ℃:

$$2ZrSiO_4 + 3Al_2O_3 — 3Al_2O_3 \bullet 2SiO_2 + 2ZrO_2 \qquad (1)$$

Yet, when conventional reaction sintering methods are employed, problems are encountered in the form of low bulk and grain boundary diffusion coefficient of mullite, and high processing temperatures (up to 1500 ℃). As a result, sintering additives such as CaO, MgO, TiO_2 and CeO, SrO are utilized to develop a transient liquid phase to produce a tough mullite- zirconia composite with high density [15-19]. Accordingly, a new sintering method for ZrO_2-mullite composite preparation is needed in order to get fully densified ZrO_2-mullite composites at relatively low temperatures, and spark plasma sintering (SPS) is an attractive choice.

Spark plasma sintering (SPS) is a new sintering process, which is capable of sintering ceramic powders quickly to its full density at a relatively lower temperature, compared to the conventional sintering methods [20-25]. Detailed configuration of the process can be found in a previous report [26]. In this process, a graphite die set is filled with the raw powder, and placed between the lower and upper electrodes. A pressure is then applied and held onto the compact during sintering. An external power source provides pulsed discharge to activate the surface of the particles. The power supply is then switched to resistance heating for densification. Charging and discharging the intervals between powder particles with electrical energy effectively generate high temperature spark plasma. SPS systems can offer many advantages over conventional sintering systems, including ease of operation and accurate control of sintering energy as well as high sintering speed, high reproducibility, safety and reliability. The SPS features a very high thermal efficiency because of the direct heating of the sintering graphite mold and stacked powder materials by the large spark pulse current. It can easily consolidate a homogeneous, high-quality sintered compact because of the uniform heating, surface purification and activation made by dispersing the spark points. There are several expected merits of SPS: 1. generation of spark plasma; 2. effect of electric current on diffusion in conductor or skin current on the semiconductor and insulator; 3. rapid Joule heating for conductors and rapid cooling.

In conventional electrical resistance hot pressing, the main factors promoting sintering are the Joule heating generated by electrical resistance, and the plastic flow of materials due to the applied pressure. Conversely, in SPS sintering, apart from these factors, the dc

pulse effectively discharges at the initial stage of sintering. The high-temperature sputtering phenomenon generated by spark plasma and spark impact pressure eliminates absorptive gas and impurities present on the surface of the powder particles. The graphite die and punches are subject to Joule heating. They function as heating elements to maintain a homogeneous sintering temperature. The presence of an electrical field causes high-speed diffusion due to the high-speed migration of ions in the plasma and the molten ceramic surfaces, which is discussed by other authors in detail [26].

The aforementioned advantages of SPS over the conventional sintering processes have prompted some studies on the application of SPS on reaction sintering of ZrO_2-mullite composites. Rocha-Rangel et al. has reported SPS of Al_2O_3-$ZrSiO_4$ powder with TiO_2 or MgO as additives [27,28]. It was found that at sintering temperatures as low as 1380 and 1420 ℃, high density (>99.5% relative density) was accomplished and the K_{IC} for the component improved to 4.91 and 5.7 MPa $m^{1/2}$, respectively. The SPS processing of $ZrSiO_4$-Al_2O_3-Al mixture to get the reaction sintered ZrO_2- mullite composites [29-31] was also attempted. In this approach, the powder mixture was initially pre-heated to 1100 ℃ to oxidize the Al. Nonetheless, the final sintering temperature as high as 1380 ℃ was still required, and post isothermal reaction treatment at 1500 ℃ was necessary for a well-densified, fully mullitized body. This was due to the low bulk and grain boundary diffusion coefficient of mullite.

In order to reduce the diffusion distances and increase the driving force for sintering, plasma spheroidization (PS) was adopted to prepare zircon-alumina mixture with fine particle size and high sintering activity [32,33].

Plasma spray technology has become an important tool for various industries, such as aerospace, auto-motive, chemical, energy and biomedical to satisfy numerous practical surface engineering exigencies. Most commercial DC plasma guns operate at 10-90 kW, with exit temperatures of the plasma exceeding 20,000 K. This approach enables rapid solidification rates of $\sim 10^6$ K s^{-1}. Plasma spheroidization (PS) directs a stream of high velocity, molten particles from a plasma jet into distilled water. Under certain conditions the mixtures coalesce in-flight, and resultant spheroidized powders are formed by rapid solidification of the individual droplets. The high cooling rate tends to result in supersaturated solid solutions with non-equilibrium phases, which is highly activated. In a previous study, it was found that the zircon-alumina powder prepared by plasma spray spheroidization has a primary mullite formation temperature of around 1000 ℃ [34].

In this study, high purity Al_2O_3 and $ZrSiO_4$ powder mixture is plasma sprayed into distilled water to form fine spherical powders that composed essentially of homogenous solid mixtures of alumina and partially dissociated zircon. A portion of zircon in the plasma-spheroidized powders is partially dissociated into zirconia and silica, while the rest remains as zircon. The mixture is then sintered by SPS without additives at different temperatures for 10 and 30 min. The microstructure and mechanical properties is investigated and discussed.

2. EXPERIMENTAL PROCEDURE

The starting materials were high purity $ZrSiO_4$ (99%), Al_2O_3 (99.99%) powders with particle sizes of 5-10 μm (Cerac Incorporated, USA). Mixtures of $ZrSiO_4$ and Al_2O_3 powders with Al_2O_3: SiO_2 molar ratios of 3:2 were milled with zirconia ball milling media using the Fritsch P-5 Planetary Mill (Fritsch GmbH, Germany). The powder to ball ratio was kept to 1:20 by weight. The bowl was put on the mill and rotated at 200 rpm for 4 h. Spray drying, and, debinding are carried out to modify the particle shape of the ball-milled powders. Subsequently, the composite powder was plasma sprayed with a 100 kW computerized plasma system 4500 (Praxair Thermal Inc., USA) to get the plasma spheroidization of the composite powder. The composite powder was then sintered by spark plasma sintering (SPS) using the Dr. Sinter 1050 SPS (Sumitomo Coal Mining Co., Japan) equipment. The SPS was carried out at different temperatures for 10 and 30 min duration. The SPS parameters are listed in Table 2.

The microstructure development of the SPS sample is inspected by the JEOL JSM-5600LV scanning electron microscope (SEM) and JEOL JEM2120 transmission electron microscope (TEM). The Philips MPD 1880 diffractometer system is used for phase evolution characterization and crystallinity analysis of the SPS samples. The microhardness of the samples is tested by the Knoop's indentation with an applied load of 500 g and a holding time of 15 s. The Young's modulus of the samples is evaluated by the CSEM MHT microhardness tester. In this tester, just as in nanoindentation [35,36], the load and displacement are recorded continuously throughout the indentation process to produce a load-displacement curve, from which the micro-mechanical properties such as hardness and Young's modulus can be calculated. The fracture toughness of the SPS sample is determined by the indentaion fracture method using the Vicker's indentation, and is calculated from the value of crack length, microhardness and Young's modulus according to the following equation:

$$K_{IC} = 0.016 * \left(P / C_0^{3/2}\right)(E/H)^{1/2} \qquad (2)$$

where P is the load in Newtons, C_0 is the crack length in m, E is the modulus in GPa and H is the hardness in GPa.

3. RESULTS AND DISCUSSION

3.1. The effect of SPS temperature on the microstructure

Fig. 1 shows the XRD result for the SPS samples sintered at the temperature of 1000 ℃ for 10 min and 1300 ℃ for 30 min. It reveals that at a temperature as low as 1000 ℃, the decomposition of zircon commences, resulting in phases such as tetragonal zirconia (t-ZrO_2) and amorphous SiO_2 along with alumina in the sample. However, a considerable amount of zircon is still present in the sample. At the SPS temperature of 1300 ℃, the decomposition of zircon is complete, with a large amount of mullite being formed. This temperature is far below the conventional reaction sintering temperature of 1500 ℃, indicating that, with a combination of PS and SPS, the decomposition of zircon and

reaction sintering of zirconia with alumina to form mullite can take place at a relatively lower temperatures. From the XRD results, it is found that samples processed at 1000 ℃ contain the metastable tetragonal zirconia phase, which is stable at high temperatures, while samples sintered at 1300 ℃ consist of the monoclinic zirconia phase, which is stable at room temperature. This is because at low SPS temperature, the decomposition has just begun, and the size of the tetragonal zirconia precipitates is very fine, as shown later in Figs. 2(a) and 3. These fine precipitates cannot overcome the phase transformation resistance induced by the matrix during the cooling process, and the metastable phase is retained at room temperature. At high SPS temperature, as shown in Fig. 2(c) and (d), the precipitates grow, and they can overcome the phase transformation resistance during the cooling process, so a more stable phase, the monoclinic zirconia is observed at room temperature.

Fig. 2 shows the microstructure of SPS ZrO_2-mullite sintered at different temperatures. From the XRD pattern and microstructure, it can be seen that at the SPS temperatures of 1000 and 1100 ℃, the decomposition of zircon and the reaction sintering of silica with alumina to form mullite have commenced. However, the new phase formed is extremely fine-scale and the shape of original zircon agglomerate remains. At the SPS temperature of 1200 ℃, mullite grains with fine intra-granular ZrO_2 are formed. Subsequently, at the SPS temperature of 1300 ℃, long-range atomic diffusion in the compact results in the re-crystallization of the newly formed phases ZrO_2 and mullite grains. The re-crystallization and grain growth is so conspicuous that no semblance of the original zircon-alumina agglomerates remained, and there are appreciable amounts of inter-granular micro-cracks and micro-pores found in the samples. From these results, it can be seen that with optimized processing parameters, SPS can yield very fine microstructures due to the rapid heating and cooling process. Also it is obvious that a combination of PS and SPS can acutely reduce the decomposition temperature of zircon and, this in turn mitigate the formation temperature of mullite. Fig. 3 shows the bright field TEM image and electron diffraction pattern for the SPS ZrO_2-mullite sample SPS at 1000 ℃ for 10 min. Large amount of spheriodized zircon grains still exists and very fine zirconia precipitates can be found in the sample. High-resolution transmission electron microscope (HRTEM) picture shows that the ZrO_2 inclusion has a grain size about 10 nm embedded within an amorphous silica matrix. Electron diffraction pattern conformed the metastable tetragonal ZrO_2 phase at low SPS temperatures. Figs. 4 and 5 show the bright field TEM image and electron diffraction pattern for ZrO_2- mullite sample SPS at 1300 ℃ for 10 min. The results show that at SPS temperature of 1300 ℃, the mullitization reaction has completed, resulting in zirconia embedded within the mullite-based composite structure. And the zirconia has coarsened. Upon subsequent cooling, it has now transformed to the stable phase, as monoclinic zirconia. Also, from the electron diffraction pattern, it can be seen that occasional residual alumina grains can still be located in the sample.

3.2. Mechanical properties of SPS ZrO2-mullite

Fig. 6 shows the Knoop's hardness results for the SPS ZrO_2-mullite samples. The typical Vicker's indentation mark with cracking on the tips for fracture toughness measurement is shown in Fig. 7. The average micro-hardness and the Young's modulus

as well as the fracture toughness for the samples are shown in Table 3. It shows that the microhardness and fracture toughness of the ZrO_2 composites increases with increasing SPS treatment temperature. At the SPS temperature of 1200 ℃, the sample has the highest microhardness and Young's modulus values, with a microhardness of HV 1266±80 and a Young's modulus of 208±27 GPa. The microhardness and Young's modulus values decrease slightly at the SPS temperature of 1300 ℃. This is because, at the SPS temperature of 1200 ℃, the densification of the sample by the SPS reaction sintering dominates the sintering process. The complete dissociation of remnant zircon in the powder mixture at this temperature contributed significantly to the formation of mullite grains along with fine-scale zirconia inclusions. The fine microstructure thus obtained in this stage gives rise to the high microhardness and fracture toughness values. However, at SPS temperatures above 1200 ℃, rapid re-crystallization and grain coarsening take place. As a result, the microhardness and Young's modulus decrease. At the SPS temperature of 1300 ℃, a notable increase of fracture toughness is observed. The fracture toughness for the sample SPS at 1300 ℃ for 30min is 10.0 ± 0.73 MPa $m^{1/2}$, and that for the sample SPS at 1300 ℃ for 10 min is 11.2 ± 1.1 MPa $m^{1/2.}$ This can also be attributed to the re-crystallization and grain growth at this high temperature, which can provide a better intergranular bonding and toughening. The formation of numerous intergranular micro-cracks can also contribute to the increase of fracture toughness.

4. CONCLUSIONS

This study confirmed that mullite-zirconia ceramic composites with attractive mechanical properties are obtained by reaction sintering of zircon-Al_2O_3 mixture at a relatively low sintering temperature using a process combining plasma spheroidization (PS) and spark plasma sintering (SPS). Subsequent microstructure and mechanical property inspection indicates that, at the SPS temperature of 1000 ℃, the decomposition of zircon begins, while at the SPS temperature of 1200 ℃, the mullite formation dominates the process, resulting in a great improvement of microhardness, Young's modulus, and toughness. A microhardness of HV 1250 ± 80, a Young's modulus of 208 ± 27 GPa, and a fracture toughness of 5.49 ± 0.82 MPa $m^{1/2}$ is obtained at this SPS temperature with a soaking time of 30 min. At the SPS temperature of 1300 ℃, due to the re-crystallization, rapid grain growth, and intergranular micro cracking, there is a slight decrease of microhard-ness and Young's modulus. Yet, it is found that a fracture toughness as high as 11.2 MPa $m^{1/2}$ is obtained at this SPS temperature. This led to the conclusion that with optimized sintering parameters, a combination of PS and SPS is an effective material-processing route for preparing mullite/ZrO2 composites with attractive mechanical properties from zircon/alumina mixture at a relatively low reaction sintering temperature.

ACKNOWLEDGEMENTS

The authors are grateful for the financial support from Nanyang Technological University in the form of research grant RG78/98.

REFERENCES

[1] R. Torrecillas, G. Fantozzi, S. De Aza, J.S. Moya, Acta Mater. 45 (3) (1997) 897-906.

[2] I.A. Askay, D.M. Dabbs, M. Sarikaya, J. Am. Ceram. Soc. 74 (1991) 2343-2358.

[3] T.I. Mah, K.S. Mazdiyasni, J. Am. Ceram. Soc. 66 (1983) 699-703.

[4] R.R. Tummala, J. Am. Ceram. Soc. 74 (5) (1991) 895.

[5] E.A. Giess, J.M. Roldan, P.J. Bailey, E. Goo, Microstructure and dielectric properties of mullite ceramics, in: K.M. Nair, R.C. Pohanka, R.C. Buchanan (Eds.), Ceramic Transactions, Microelectronic Systems, vol. 15, American Ceramic Society, Westerville, OH, 1990, pp. 167-172.

[6] S. Kanzaki, M. Ohashi, H. Tabata, T. Kurihara, S.-I. Iwai, S.-I. Wakabayashi, Mullite-silica ceramics for insulating substrate materials, in: S. Somiya, R.F. Davis, J.A. Pask (Eds.), Ceramic Transactions. Mullite and Mullite Matrix Composites, vol. 6, American Ceramic Society, Westerville, OH, 1990, pp. 389-399.

[7] N. Claussen, J. Jahn, J. Am. Ceram. Soc. 63 (1980) 228-229.

[8] K.A. Khor, Y. Li, Mater. Sci. Eng. A256 (1998) 271-279.

[9] J.S. Moya, M.I. Osendi, J. Mater. Sci. Lett. 2 (1983) 599-601.

[10] E. Di Rupo, M.R. Anseau, R.J. Brook, J. Mater. Sci. 14 (1979) 2924-2928.

[11] M. Holstrom, T. Chartier, P. Boch, Mater. Sci. Eng. A109 (1989) 105-109.

[12] J.S. Wallace, N. Claussen, M. Ruhle, G. Petzow, Development of phases in in-situ-reacted mullite-zirconia composites, in: J. Park, A.G. Evans (Eds.), Ceramics and Ceramic-Metal Interfaces, Plenum, New York, 1981, pp. 155-165.

[13] P. Boch, J.P. Giry, Mater. Sci. Eng. 71 (1985) 39-48.

[14] M.R. Anseau, C. Leblud, F. Cambier, J. Mater. Sci. Lett. 2 (1983) 366-370.

[15] P. Pena, P. Miranzo, J.S. Moya, S. De Aza, J. Mater. Sci. 20 (1985) 2011-2022.

[16] K. Das, S.K. Das, B. Muhkerjee, G. Banerjee, Int. Ceram. Rev. 47 (5) (1998) 304.

[17] J.M. Rincon, J.S. Moya, Brit. Ceram. Trans. J. 85 (1986) 201-/206.

[18] S. Kinikoglu, M. Marsoglu, J. Eur. Ceram. Soc. 14 (1994) 45-51.

[19] K. Das, B. Mukherjee, G. Banerjee, J. Eur. Ceram. Soc. 18 (12) (1998) 1771-1777.

[20] D.L. Johnson, Ceram. Int. 17 (5) (1991) 295-300.

[21] S.H. Risbud, C.H. Shan, Mater. Sci. Eng. A204 (1995) 146-151.

[22] H. Su, D.L. Johnson, J. Am. Ceram. Soc. 79 (12) (1996) 3199- 3201.

[23] J. Hong, L. Gao, S.D.D.L. Torre, H. Miyamoto, K. Miyamoto, Mater. Lett. 43 (2000) 27-31.

[24] C.H. Shan, S.H. Risbud, Mater. Sci. Eng. B26 (1994) 55-60.

[25] L. Gao, H.Z. Wang, J.S. Hong, H. Miyamoto, K. Miyamoto, Y. Nishikawa, S.D. de la Torre, Nanostruct. Mater. 11 (2) (1999) 43-49.

[26] J.R. Groza, A. Zavaliangos, Mater. Sci. Eng. A287 (2000) 171-177.

[27] E. Rocha-Rangel, H. Balmori-Ramirez, S.D. de la Torre, H. Miyamoto, M. Umetomo, K. Tsuchiya, Spark plasma sintering of mullite-zirconia-TiO_2 ceramics. Ceramic Engineering and Science Proceeding, 24th Annual Conference on Composites, Advanced Ceramics, Materials and Structures: B Jan 23-Jan 28, 2000, vol. 21, no. 4, Cocoa Beach, FL, pp. 95-102.

[28] E. Rocha-Rangel, S.D. de la Torre, H. Miyamoto, M. Umemoto, K. Tsuchiya, H. Balmori-Ramirez, Processing and properties of mullite-ZrO_2 prepared by RS and SPS routes with additions of MgO, in: N.P. Bansal, J.P. Singh, E. Ustundag (Eds.), Advances in Ceramic-Matrix Composites V, The American Ceramic Society, Westerville, OH, pp. 75-83.
[29] S.D. de la Torre, H. Miyamoto, K. Miyamoto, J. Hong, L. Gao, L. Tinoco-D., E. Rocha-Rangel, H. Balmori-Ramirez, Spark plasma sintering of nano-composite ceramics. 6th International Symposium on Ceramic Materials and Components for Engineering, October 19-23, 1997, Arita, Japan, pp. 892-897.
[30] E. Rocha-Rangel, S.D. de la Torre, H. Balmori-Ramirez, Ceram. Trans. 115 (2000) 285-292.
[31] E. Rocha-Rangel, S.D. de la Torre, H. Miyamoto, M. Umemoto, K. Tsuchiya, J.G. Cabanas-Moreno, H. Balmori-Ramirez, Ceram. Trans. 94 (1999) 91-96.
[32] K.A. Khor, Y. Li, Mullite-Zirconia Composites Prepared by Plasma Spraying of Zircon and Alumina Mixtures, Materials and Manufacturing Processes, vol. 14(5), Marcel Dekker, New York, 1999, pp. 661-678.
[33] K.A. Khor, Y. Li, Mater. Lett. 48 (2) (2001) 57-63.
[34] Y. Li, K.A. Khor, J. Mater. Technol. 89-99 (1999) 532-537.
[35] C. Brun, P. Delobelle, M. Fromm, F. Berger, A. Chambauder, F. Jaffiol, Mater. Sci. Eng. A315 (2001) 63-69.
[36] G.E. Fougere, L. Riester, M. Ferber, J.R. Weertman, R.W. Siegel, Young's modulus of nanocrystalline measured by nanoindentation, Mater. Sci. Eng. A204 (1995) 1-6.

List of Figures

List of Tables

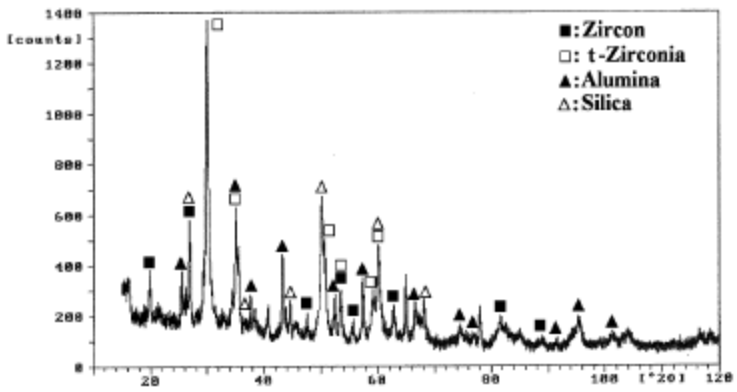
■:Zircon
□: t-Zirconia
▲:Alumina
△:Silica
[counts]
1400
1200
1000
800
600
400
200
0
20
40
60
80
100
[°2θ]
120

(a)

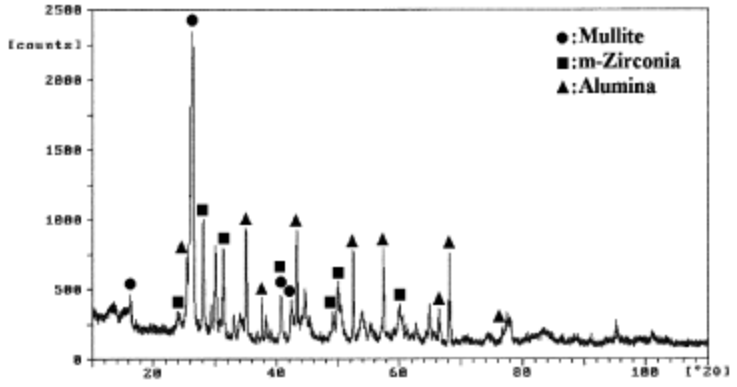
●:Mullite
■:m-Zirconia
▲:Alumina
[counts]
2500
2000
1500
1000
500
0
20
40
60
80
100
[°2θ]

(b)

Figure 1

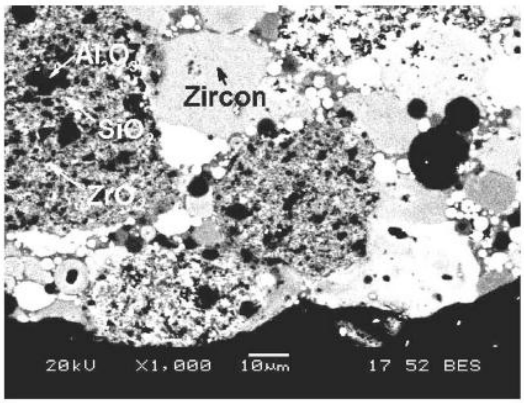

(a) SPS at 1000 °C for 10 minutes

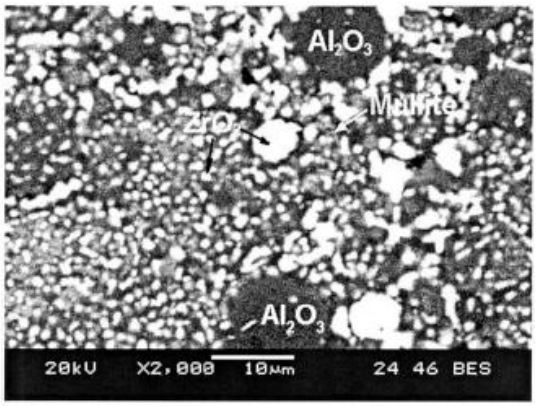

(c) SPS at 1200 °C for 30 minutes.

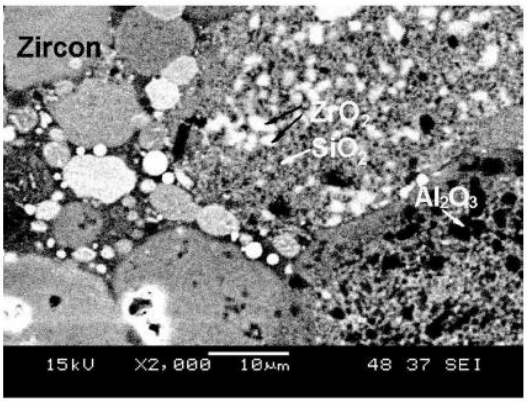

(b) SPS at 1100 °C for 30 minutes

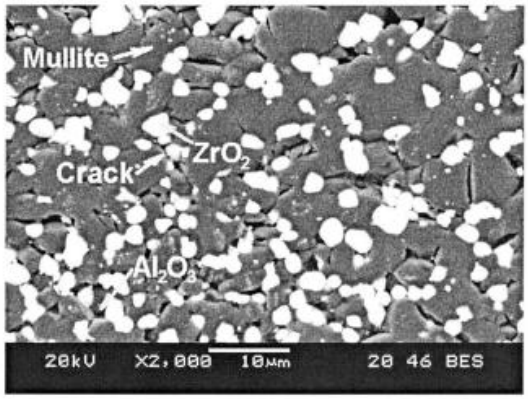

(d) SPS at 1300 °C for 10 minutes

Figure 2

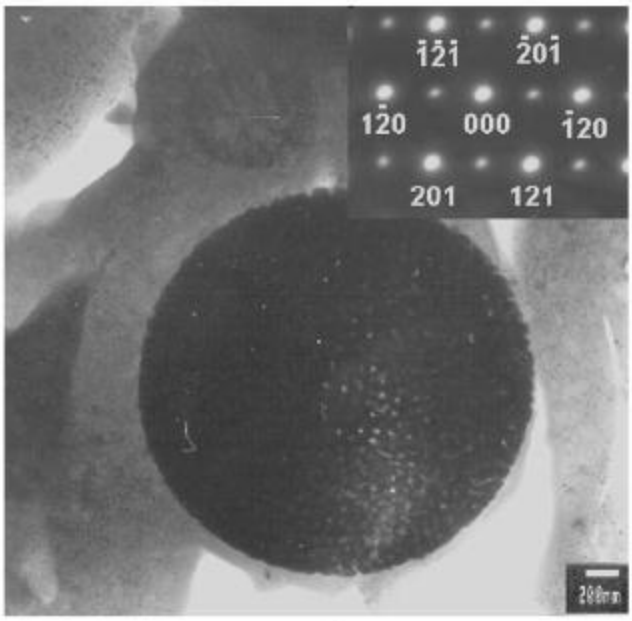
$\bar{1}2\bar{1}$
$\bar{2}0\bar{1}$
$\bar{1}\bar{2}0$
000
$\bar{1}20$
201
121
200nm

(a)

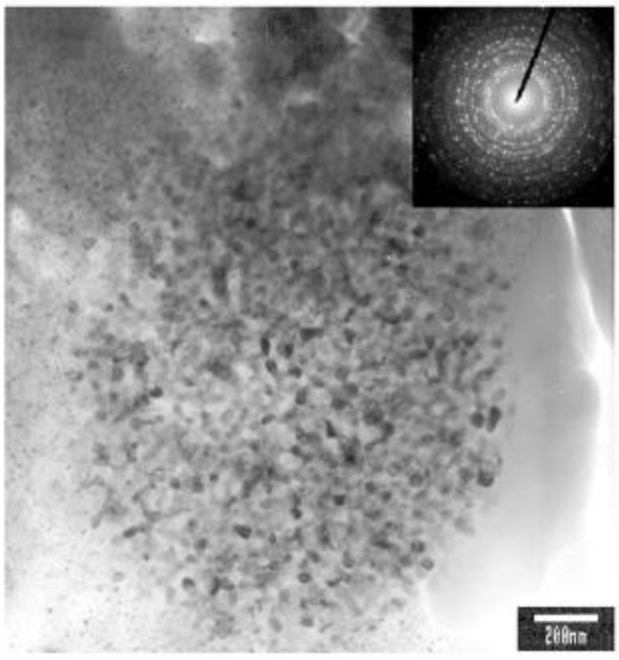
200nm

(b)

Figure 3

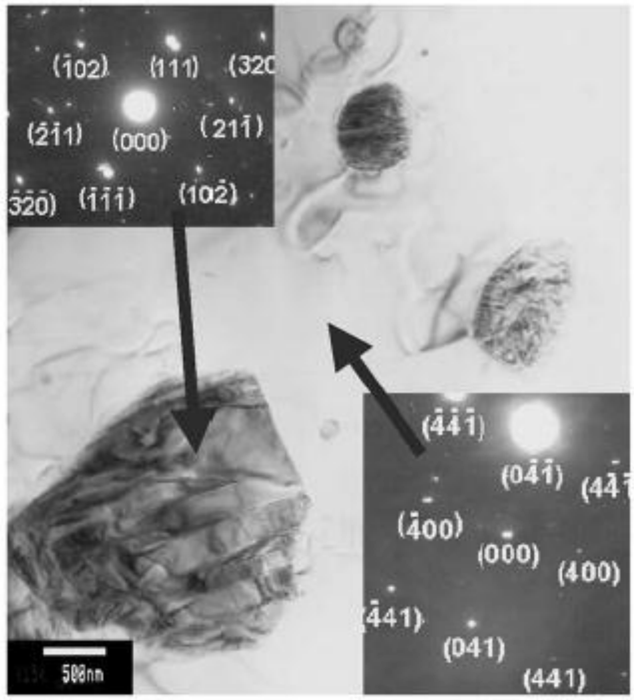
($\bar{1}02$)
(111)
(320
($\bar{2}\bar{1}1$)
(000)
($21\bar{1}$)
$\bar{3}\bar{2}0$)
($\bar{1}\bar{1}\bar{1}$)
($10\bar{2}$)
($\bar{4}\bar{4}\bar{1}$)
($0\bar{4}\bar{1}$)
($4\bar{4}$
($\bar{4}00$)
(000)
(400)
$\bar{4}41$)
(041)
(441)
500nm

(a)

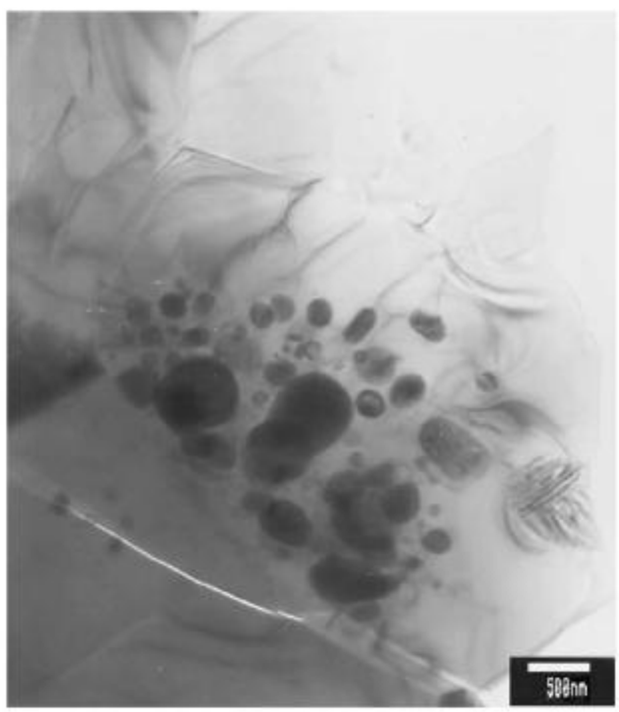
500nm

(b)

Figure 4

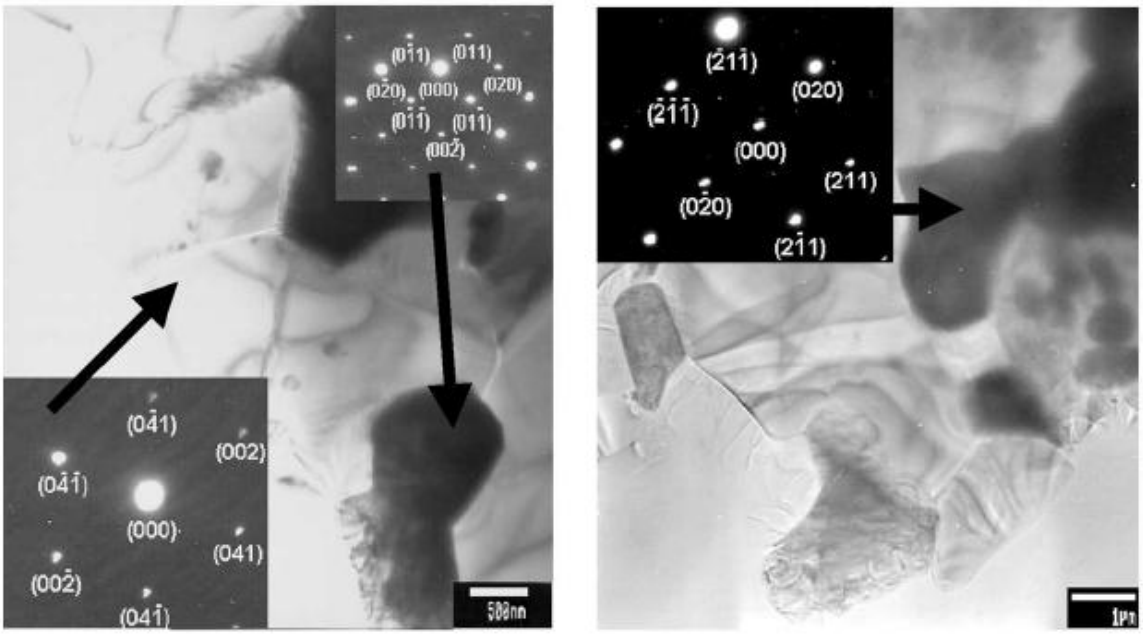

(a) mullite from [100] zone axis and ZrO_2 from [100] zone axis (b) ZrO_2 from $[10\bar{2}]$ zone axis

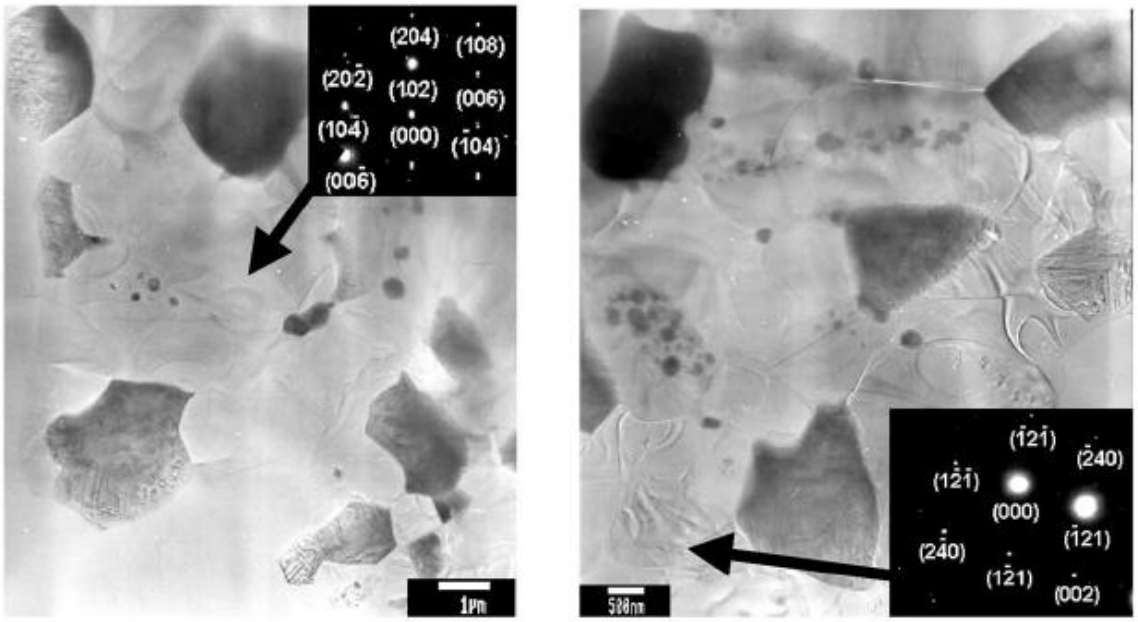

(a) Mullite from [010] zone axis (d) Alumina from [210] zone axis

Figure 5

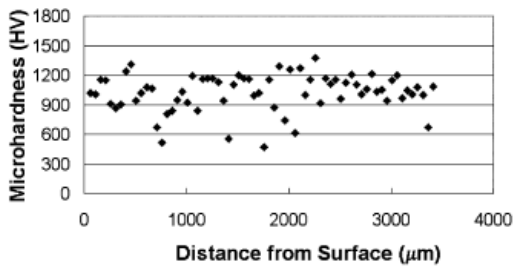

(a) Sample ZAS 1

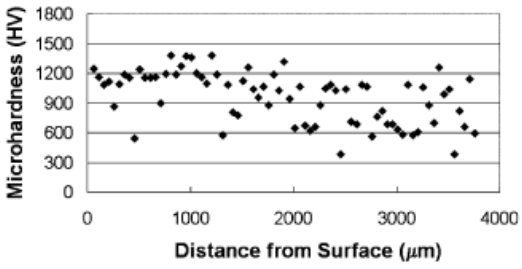

(b) Sample ZAS2

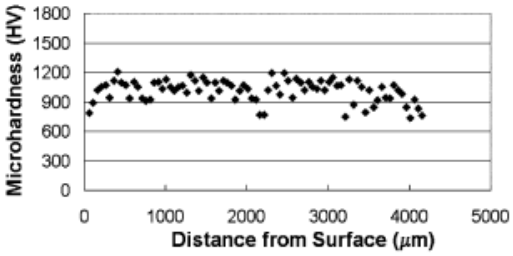

(c) Sample ZAS 3

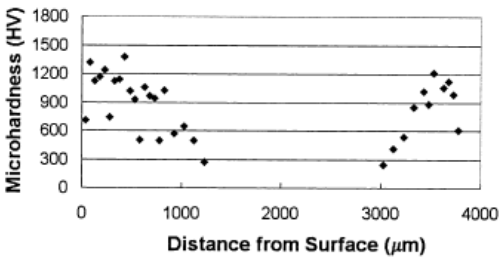

(d) Sample ZAS 4.

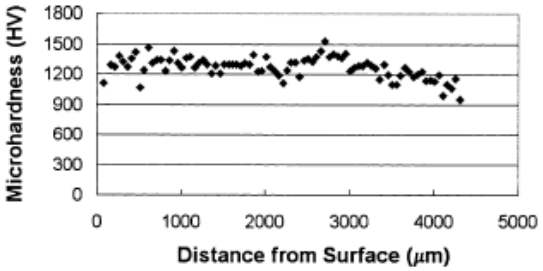

(e) Sample ZAS 6.

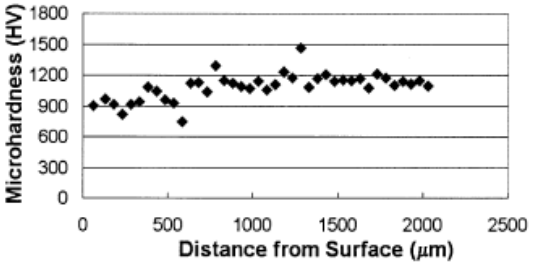

(f) Sample ZAS 7

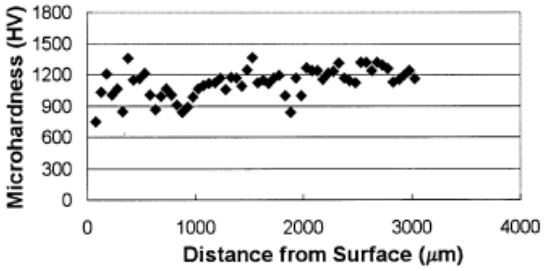

(g) Sample ZAS 5

Figure 6

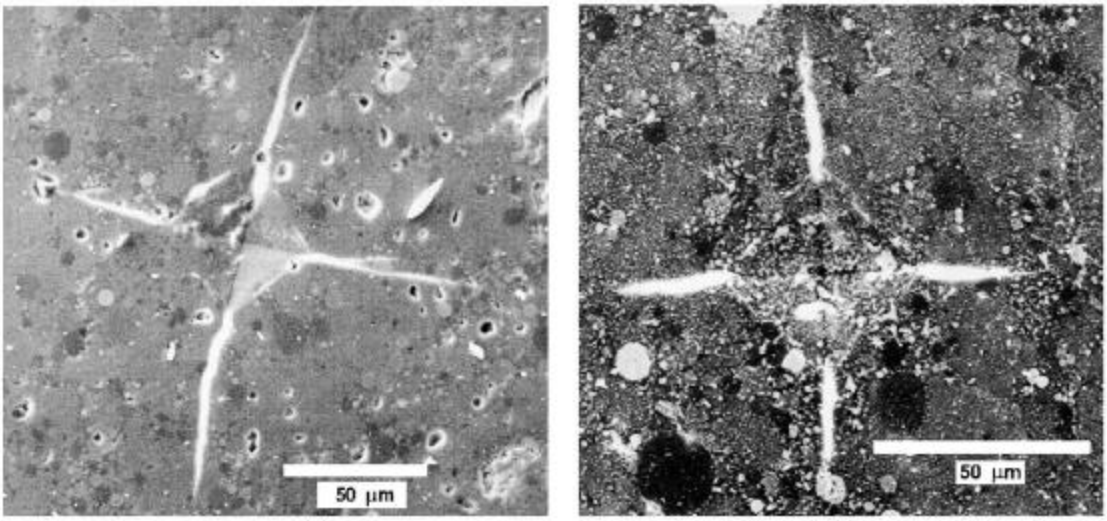

(a) (b)

Figure 7

Material	Mullite	Yttria stabilized zirconia (YSZ)	Alumina
Young's modulus (GPa)	150	200	200
Poisson's ratio	0.25	0.23	0.22
Fracture toughness (MPa $m^{1/2}$)	2	13	4–5
Micro-hardness (Knoop 1000 g, GPa)	7.4	12.7	11–14

Table 1

Sample	Temperature (°C)	Soaking Time (min)
ZAS 1	1000	30
ZAS 2	1000	10
ZAS 3	1100	30
ZAS 4	1100	10
ZAS 6	1200	30
ZAS 5	1300	30
ZAS 7	1300	10

Table 2

Sample	Knoop's hardness H_K (Kgf mm^{-2})	Young's modulus E (GPa)	Toughness K_{IC} (MPa m$^{1/2}$)
ZAS 1	1024±150	186±7	3.77±0.29
ZAS 2	960±220	146±26	3.59±0.83
ZAS 3	1012±90	167±17	4.61±0.56
ZAS 4	986±140	135±6	2.51±0.53
ZAS 6	1266±80	208±27	5.49±0.82
ZAS 5	1124±110	189±21	10.00±0.73
ZAS 7	1089±90	203±25	11.21±1.09

Table 3